Improvements in analysis techniques for segmented mirror arrays

Gregory J. Michels*, Victor L. Genberg, Gary R. Bisson
Sigmadyne, 803 West Ave, Rochester, NY 14611
*michels@sigmadyne.com (585)235-6892

ABSTRACT

The employment of actively controlled segmented mirror architectures has become increasingly common in the development of current astronomical telescopes. Optomechanical analysis of such hardware presents unique issues compared to that of monolithic mirror designs. The work presented here is a review of current capabilities and improvements in the methodology of the analysis of mechanically induced surface deformation of such systems. The recent improvements include capability to differentiate surface deformation at the array and segment level. This differentiation allowing surface deformation analysis at each individual segment level offers useful insight into the mechanical behavior of the segments that is unavailable by analysis solely at the parent array level. In addition, capability to characterize the full displacement vector deformation of collections of points allows analysis of mechanical disturbance predictions of assembly interfaces relative to other assembly interfaces. This capability, called racking analysis, allows engineers to develop designs for segment-to-segment phasing performance in assembly integration, 0g release, and thermal stability of operation. The performance predicted by racking has the advantage of being comparable to the measurements used in assembly of hardware. Approaches to all of the above issues are presented and demonstrated by example with SigFit, a commercially available tool integrating mechanical analysis with optical analysis.

Keywords: Finite Element, Active Control, Segment, Surface Deformation, Optomechanical, Racking

1. INTRODUCTION

Increasing performance requirements in high precision astronomical instruments have created the need for increased capability in predicting their performance when subjected to operational environments. Both ground based and space based environments contain thermal variations and vibration disturbances that must be considered in the design development of such high precision systems. Figure 1 shows a flow chart of analysis capabilities.[1,2]

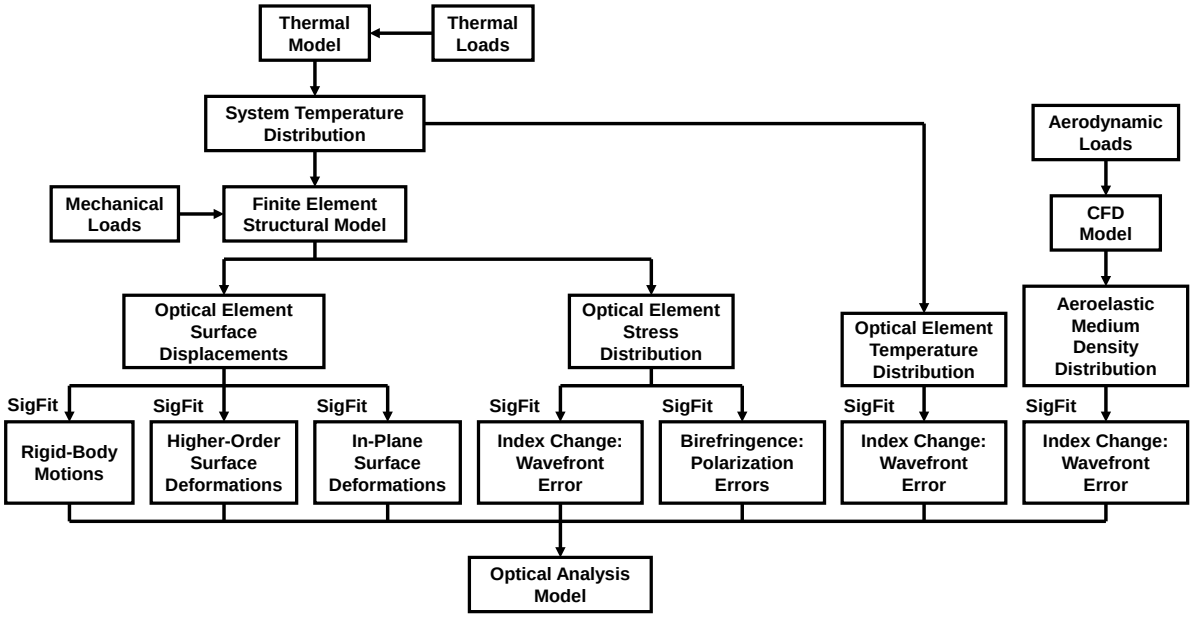

Figure 1. Flow chart of integrated optomechanical analysis capabilities.

As shown in Figure 1 disturbances are primarily caused by three physical phenomena: surface deformation, refractive index changes due to stresses in transmissive optics, and refractive index changes due to temperature changes in transmissive optics. In addition, optical performance can be affected by density variations of the aeroelastic medium around and optical system such as may be encountered in aeronautical applications.

1.1 Analysis Challenges of Segmented Surfaces

Segmented astronomical systems such as that shown in Figure 2 present unique analysis challenges relative to other systems. Behavior of the array as a single surface is characterized by discontinuous behavior between segments. This presents challenges in describing surface deformations. In addition, surface deformations can be expressed relative to an absolute coordinate system, the average motion of the segment array (also referred to as the parent surface), or each individual segment. Furthermore, in some cases it is of interest to know the surface deformation of each segment relative to a mounting interface plane. Likewise, prediction of the line-of-sight (LOS) error due to vibration response is complicated by the fact that each segment acts to add its own contribution to the system LOS error.

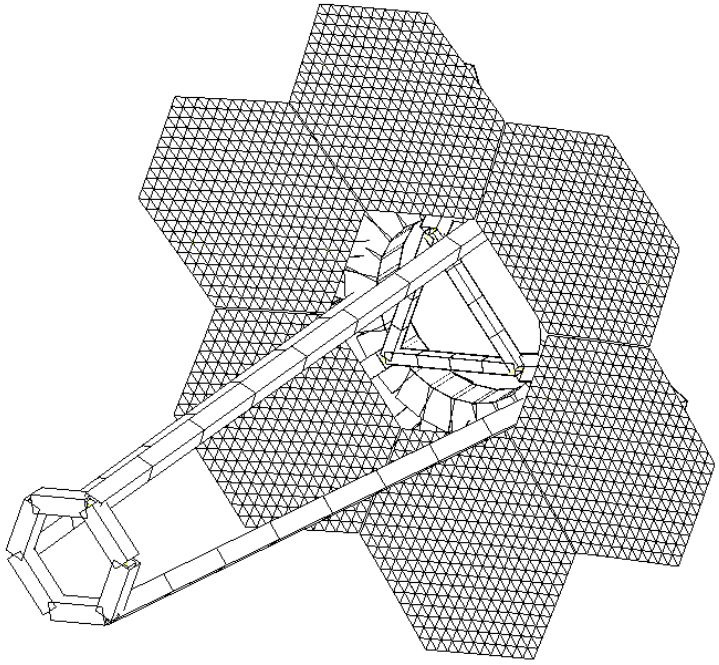

Figure 2: Finite element model of an example segmented astronomical telescope.

Moreover, design engineers are also often interested in the motion and deformation of the mount interface points of each segment. Such predictions, referred to as racking, may also be cast relative to the parent level behavior of the whole array, relative to a key mounting interface location, or relative to the segment average motion. Such analysis can be used to express deformations in a way that is comparable to measured test data in support of assembly of a segmented system.

Therefore, specialized analysis techniques must be employed in order to arrive at analysis results useful for comparison to design requirements.

2. OPTOMECHANICAL ANALYSIS OF SEGMENTED SYSTEMS

2.1 Surface Deformation Analysis of Segmented Optics

Analysis of surface deformation analysis of segmented optics can be demonstrated by considering a gravity deformation analysis of the finite element model of the example segmented system shown in Figure 2. Gravity was applied along the optical axis, and the results were processed in SigFit. [3] The results shown in Figure 3(a) are the surface deformation of the array with the rigid body motion of the full parent surface subtracted. The residual deformation is characterized by

tilt of each segment. Figure 3(b) shows the surface deformation after power at the parent level is subtracted. The results would suggest that each segment is elastically deforming with power and coma. However, these results are actually due to lateral motions of the optics. To get a correct understanding of the elastic deformation of the segments the rigid body motions of the individual segments are subtracted from each segment, respectively, and are shown in Figure 3(c). This gives us the expected result dominated by trefoil deformation.

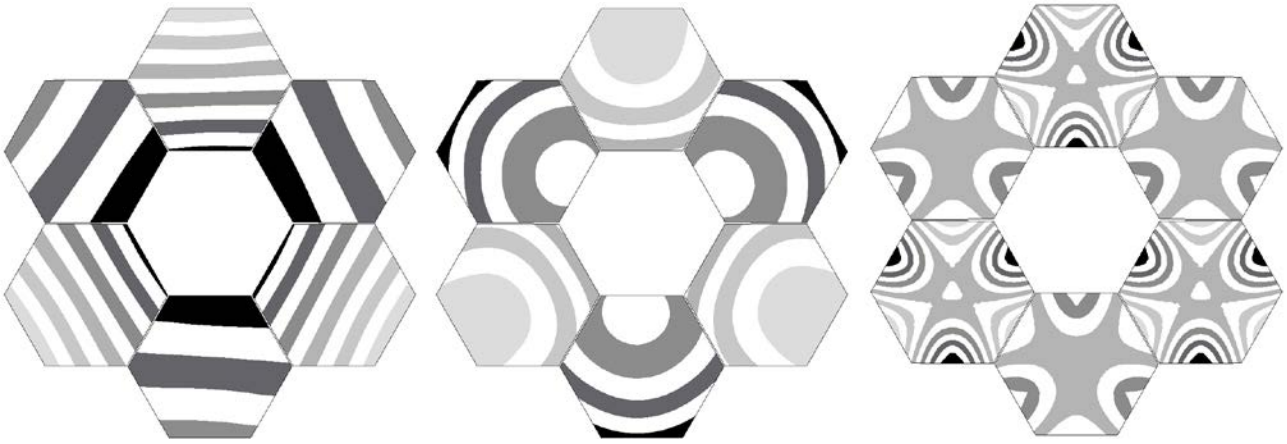

(a) (b) (c)

Figure 3: Surface deformation of a segmented array: (a) residual deformation after subtraction of parent rigid body motion, (b) residual deformation after subtraction of parent rigid body motion and parent power, and (c) residual deformation after subtraction of segment rigid body motions.

The results in Figure 3 may also be used to taget design improvement efforts. Figure 3(a) would suggest that the support structure should be redesigned because the segments at 4, 8 and 12 o'clock have more tilt than the other segments. Figure 3(b) suggests that the same segments are moving laterally more than the rest. Figure 3(c) shows that the same segments have more gravity-induced distortion, which could be due to substrate stiffness or the segment mount locations. The ability to view the same results in different ways helps the design engineer understand the optical effects due to the mechanical design. For large segmented arrays, this automated analysis capability is extremely useful in targeting efforts to improve the system level performance.

In some cases it is of interest to design engineers to understand the parent level or segment level rigid body motion with respect to different references. For example, if rigid body motion of the parent is computed by conventional means, then the results will be with respect to the fixed reference frame of the finite element analysis. This fixed reference frame will be a function of how the boundary conditions are applied in the finite element model. However, engineers often would like to know the rigid body motion and residual deformation of either the parent or the segments with respect to a critical interface plane, as shown in Figure 4, or the rigid body motion of the segments relative to the average motion of the parent.

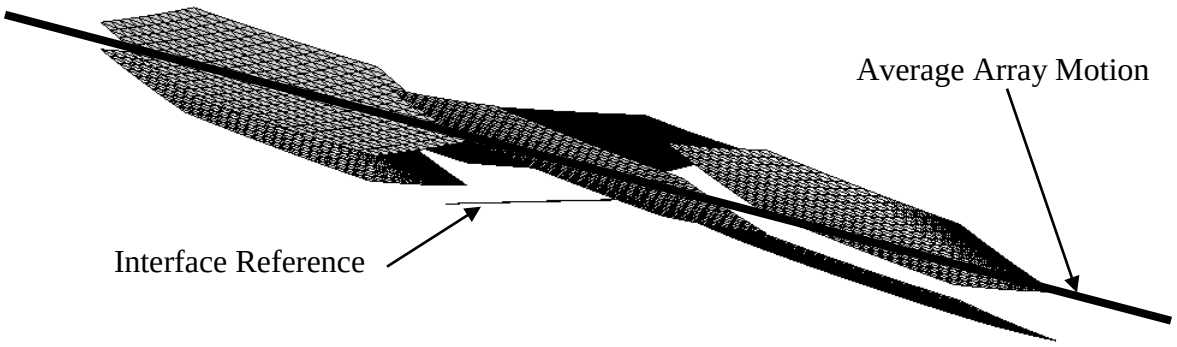

Figure 4: Prediction of a deformed segmented array showing average array motion with respect to an interface reference.

Calculation of such relative motion and residual deformation requires transformation of the nodal displacements of the segments into the convected coordinate system of the average motion of the parent.

2.2 Vibration Analysis of Segmented Optics

The previous section shows the value of segment analysis in static analysis. In vibration analysis, the tool is even more useful. Most telescopes, whether ground based or orbiting, are subjected to operational random base shake vibration input. An understanding of such a vibration environment on optical performance such as surface error and system LOS error is required. As an example, a random base shake was applied to the above simple telescope model. Two sets of surface error results are provided:

1) Parent level average motion and parent surface RMS surface error after subtraction of parent average motion
2) Individual segment motion relative to the parent and segment RMS surface error after subtraction of segment average motion

The output is similar to the static output, but is based on the vibration response due to random vibration loads. Additional output identifies the percent contribution of each mode to each performance prediction. Just as in the static example in section 2.1, the output provides information to the design engineer to help identify possible improvements to the segmented optic, such as segment mount locations or segment stiffness.

Segment analysis may also be applied to the optical performance metric of LOS error. Figure 5 shows a finite element model of a segmented telescope with individual LOS rays for each segment. Rather than looking at the relative motion of segments relative to the parent, the segment LOS calculation instead converts that motion into relative LOS pointing errors for each segment. The LOS error for each segment is quantified using the motion of each segment relative to the parent motion. It is often of interest to engineers to not only understand the parent LOS error but also the variation of LOS error from the contribution of each segment. Understanding the contribution of individual segments relative to the parent can help focus design improvement efforts in systems with many segments. This allows design engineers to address major design contributors to performance more easily.

Additionally, random response output identifies the percent contribution of each mode to the LOS response. This allows engineers to augment their insight with focus on specific significantly contributing modes. For example, Table 1 shows that mode 17 is the most significantly contributing mode to the translational LOS error, labeled LI-TV. Figure 5 shows a deformed plot of mode 17. A design engineer could also plot the strain energy density in this mode to determine areas of possible design improvement.

Table 1: Percent Modal Contributions of LOS Error

Each modes % contribution to LoS JITTER PSD

Mode	Freq	LI-TX	LI-TY	LI-TV	LI-RX	LI-RY	LI-RV	LO-RX	LO-RY	LO-RV
4	25.50	14.603	0.000	1.668	0.044	8.198	1.095	0.000	14.603	1.668
5	25.50	0.004	18.128	16.058	11.682	2.834	10.541	18.128	0.004	16.058
6	59.79	0.749	0.013	0.097	0.006	0.526	0.073	0.013	0.749	0.097
7	59.79	20.230	19.473	19.559	15.705	7.520	14.650	19.473	20.230	19.559
8	62.15	0.000	0.000	0.000	0.000	0.000	0.000	0.000	0.000	0.000
9	79.16	0.000	0.000	0.000	0.000	0.000	0.000	0.000	0.000	0.000
10	90.33	0.002	0.000	0.000	0.000	0.002	0.000	0.000	0.002	0.000
11	90.33	14.462	20.347	19.675	16.712	8.590	15.665	20.347	14.462	19.675
12	92.96	0.000	0.000	0.000	0.000	0.000	0.000	0.000	0.000	0.000
13	96.30	0.227	7.356	6.542	3.866	0.430	3.423	7.356	0.227	6.542
14	96.31	0.131	0.000	0.015	0.000	0.060	0.008	0.000	0.131	0.015
15	103.69	0.000	0.000	0.000	0.000	0.000	0.000	0.000	0.000	0.000
16	114.54	32.257	0.125	3.795	0.019	41.306	5.342	0.125	32.257	3.795
17	114.54	7.935	33.959	30.987	49.906	1.023	43.604	33.959	7.935	30.987

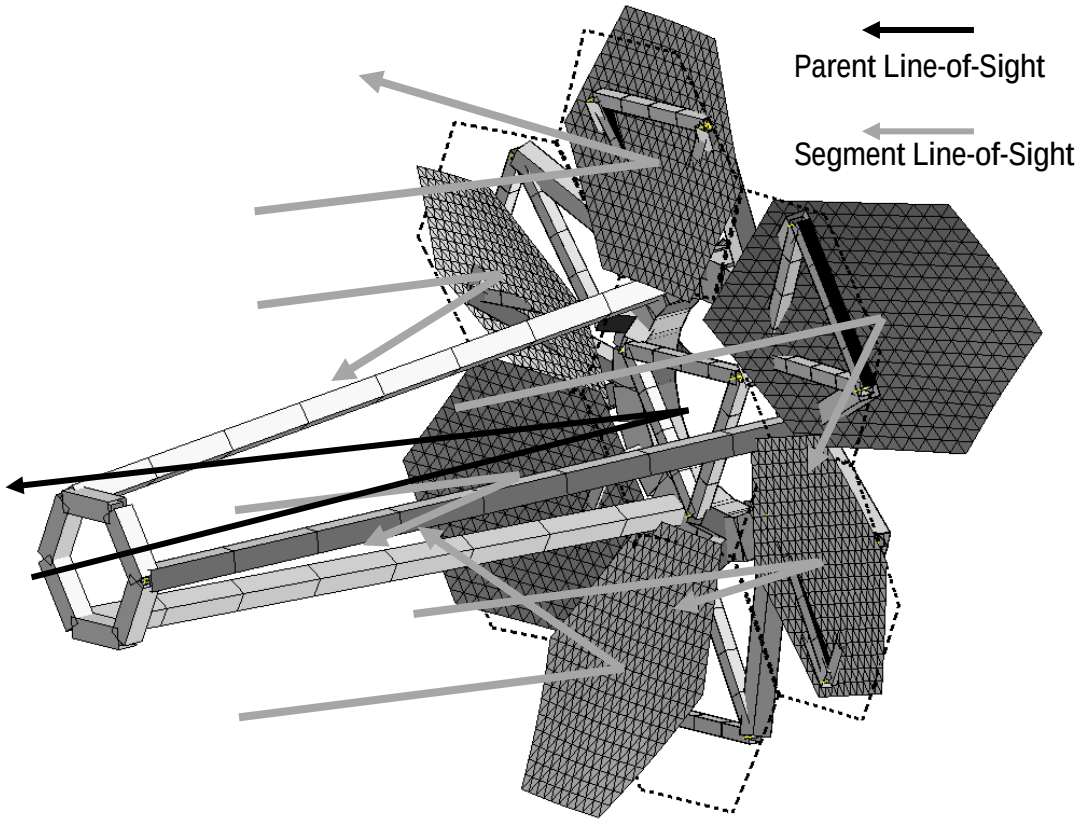

Figure 5: Illustration of segment lines-of-sight shown in grey and parent line of sight shown in black.

Table 2 provides the average parent LOS and the segment relative delta away from the average parent LOS. In this example segments 4 and 6 are the most significant LOS error contributors.

Table 2: Random response of LOS error. Segment values are relative to parent.

	Line-of-Sight Error on Image (micrometers)
Parent	22.9
Segment 1	53.9
Segment 2	56.5
Segment 3	55.1
Segment 4	108.7
Segment 5	67.1
Segment 6	149.7

3. RACKING ANALYSIS OF SEGMENTED SYSTEMS

Racking analysis is a mechanical displacement analysis that quantifies the displacements of sets of nodes with respect to a specific convected reference frame. While the racking solution definition uses the same terminology as surface fitting analysis, such as defining surfaces and segments, the algorithm is more general in its implimentation than surface

analysis. The reference can be defined using any points within the FE model. This could be a central optical element in an array, an entire optical surface, a set of assembly interface points, or a location on an existing structure at which measurement are collected. Groups of tracked nodes, typically defined as segments, may represent any objects of interest within the model. While typically these may include optical assembly interfaces they could alternatively include motor or actuator monts, interfaces to other structures, restrain locations, etc. The key is that deformations are post-processed relative to a reference defined by set of nodes that can deform and move with the structure. The output includes both the absolute and relative deformations of the tracked nodes relative to the reference system and also relative to the average behavior of the nodes' respective segment group.

3.1 Racking Analysis as a Performance Metric

Figure 6 shows an example segmented array with mount interface triads overlaying it. There is one mount interface triad for each of the six segments and one interface triad at the center representing the mount interface points of the image plane assembly mount interface. The six sets of interface points for the segments are treated as six sets of tracked nodes while the reference is defined to be the interface points of the image plane assembly.

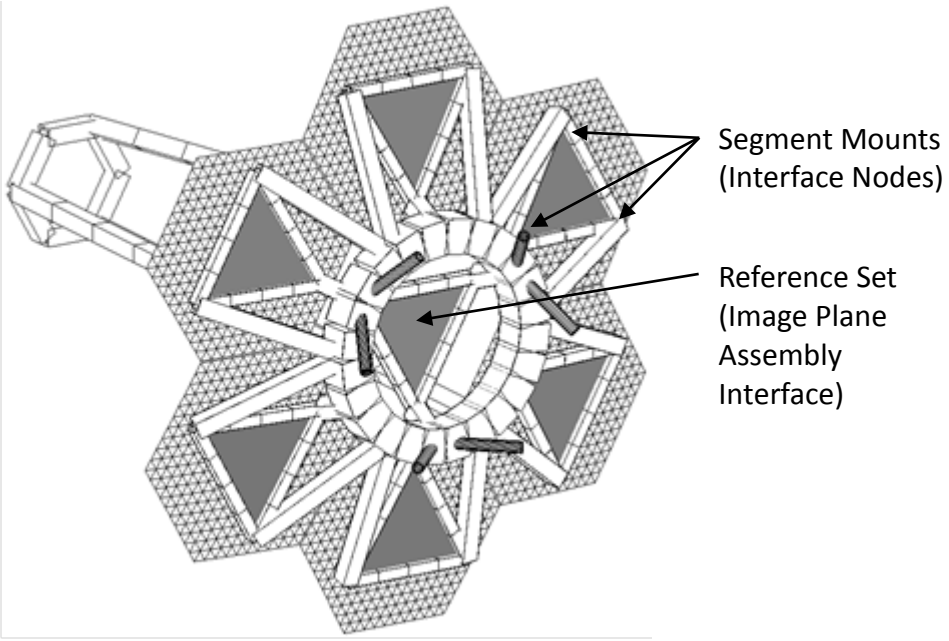

Figure 6: Finite element model of segmented array with triads of mount interface points overlain. The center triad corresponds to a reference interface with respect to which the racking output is to be expressed.

A typical finite element deformed shape plot is shown in Figure 7. Attempting to interpret the deformation in terms of how the individual segments are both moving and distorting is difficult. Notice in this figure that there is measureable rigid body motion of the reference surface interface points as well as distortion of the individual segments. If this system incorporated adaptive optics, the actuator motion required to realign the segments relative to the image plane would not include this rigid body motion of the reference plane or the racking of the individual segments. The segment racking algorithm in SigFit is the ideal tool to post-process the complex deformation set.

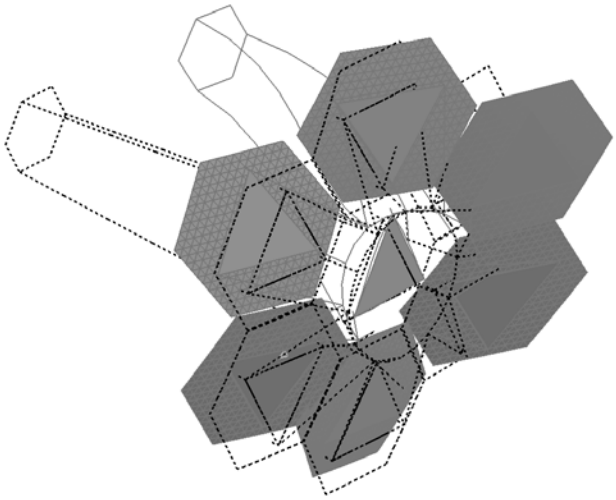

Figure 7: Deformed shape of the entire telescope due to a lateral gravity load.

In this example deformations of 21 nodes are tracked (3 image assembly mount interface plane nodes in the center of the array and 3 segment interfaces for each of the six segments). A simplified view of the unprocessed deformed shape of the 21 nodes is shown in Figure 8(a). As noted above, the total deformations include measureable rigid body motion of the reference interface points. The rigid body motion is defined as the best fit rigid body motion of the reference triad and is computed using the three translational components of deformation of the three nodes of the image assembly mount interface plane. These rigid body motions may then be subtracted from the nodal displacements of the segments through a coordinate transformation. These results are the nodal displacements of the segment interface points that result in phasing and figure errors in each segment and are shown in Figure 8(b). A further result may be obtained by subtracting the best fit rigid body motion of each segment from its respective segment nodal displacements by a similar coordinate transformation operation as was used to compute the racking results relative to the reference triad. The results, shown in Figure 8(c), are the nodal displacements responsible for the generation of figure errors in each segment.

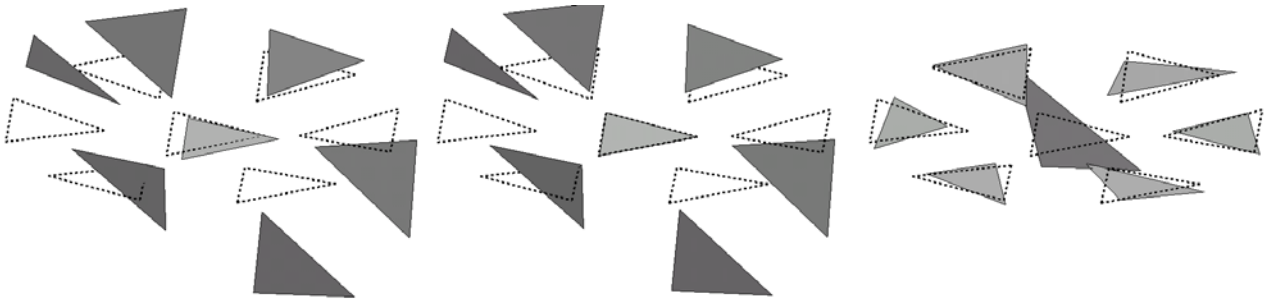

(a) (b) (c)

Figure 8: Deformations of the segment and reference interface triads with different levels of subtraction: (a) no subtraction, (b) parent level subtraction, and (c) segment level subtraction.

While the graphical representation of the example is useful, a review of the numeric results can provide additional insight into the process. The total deformations for the 21 interface nodes are shown in Table 3. Also shown in the table is the best fit rigid body motion of the reference plane. In this example it is defined as the best-fit motion of three nodes, 8101, 8105, and 8110.

Typically FE results are expressed in the displacement coordinate system of the node, which could be unique for any or all nodes, further complicating interpretation of the output. An advantage of using SigFit to post process the deformations is that results have been converted to a common displacement system that has been specified by the user.

The deformations after the subtraction of the reference plane rigid body motion are shown in Table 4. With the exception of the reference surface itself, these results include both rigid body motion and racking deformations of the individual

segments. Again, using a best-fit calculation, the rigid body motion of each segment is determined and is also shown in the table. As a check of the process, the reader should note that the rigid body motions of the reference are identically zero for this step in the process since they are removed during this reference rigid body removal operation. The deformations shown for the segments are the individual motions required for the best fit alignment of each individual segment to the reference surface. More in depth analysis involving the simulation of phasing and figure correction of adaptively controlled segmented systems can be found in references 4 and 5.

Table 3: Segment Racking - Total Deformations

Segment	Segment	NODE	Total Deformation						Rigid Body Motion of Reference					
SID	Name	ID	TX	TY	TZ	RX	RY	RZ	TX	TY	TZ	RX	RY	RZ
			in	in	in	rad	rad	rad	in	in	in	rad	rad	rad
	Focal	8101	9.1E-04	-1.2E-04	9.6E-05	5.8E-05	7.1E-05	-5.2E-06	9.1E-04	-5.9E-05	-1.4E-09	-8.6E-07	-8.5E-06	2.1E-10
	Plane	8105	8.9E-04	-2.0E-05	-1.1E-04	-3.7E-05	6.0E-05	2.1E-06						
100		8110	9.8E-04	-4.6E-05	1.2E-05	1.4E-06	1.5E-04	3.1E-06						
	SEG101	8201	1.1E-03	-2.0E-04	-3.1E-04	4.9E-05	1.2E-04	-5.5E-06						
		8205	1.4E-03	-2.8E-04	-4.4E-03	7.0E-05	1.5E-04	1.0E-05						
101		8210	1.4E-03	-2.9E-04	-1.3E-03	4.3E-05	1.4E-04	-6.0E-06						
	SEG102	8301	7.9E-04	-2.0E-04	5.6E-04	3.2E-05	6.7E-05	1.1E-05						
		8305	6.2E-04	-1.3E-04	9.8E-04	3.6E-05	3.2E-05	8.2E-06						
102		8310	6.2E-04	-4.1E-04	1.5E-03	2.4E-05	3.7E-05	1.0E-05						
	SEG103	8401	8.5E-04	-1.2E-04	2.8E-04	3.5E-06	7.6E-05	-9.3E-06						
		8405	1.3E-03	-6.5E-05	2.5E-03	4.2E-05	8.0E-05	-2.1E-05						
103		8410	1.0E-03	7.1E-05	2.7E-03	1.5E-05	9.1E-05	-5.7E-06						
	SEG104	8501	8.9E-04	1.5E-04	1.6E-03	-4.7E-05	1.1E-04	-3.6E-06						
		8505	1.1E-03	3.0E-04	3.7E-03	-7.8E-05	9.4E-05	5.9E-06						
104		8510	1.1E-03	2.9E-04	4.4E-03	-7.1E-05	1.1E-04	-1.4E-06						
	SEG105	8601	1.0E-03	2.7E-05	3.1E-05	-8.8E-06	1.4E-04	1.5E-05						
		8605	1.5E-03	-7.0E-05	1.9E-03	-4.2E-06	1.4E-04	1.1E-05						
105		8610	1.5E-03	1.7E-04	-1.4E-03	-9.1E-06	1.4E-04	1.2E-05						
	SEG106	8701	1.1E-03	-1.1E-04	-2.2E-03	3.3E-05	1.6E-04	-7.7E-06						
		8705	1.2E-03	-2.9E-04	-4.7E-03	3.3E-05	1.6E-04	-1.4E-05						
106		8710	1.5E-03	-4.4E-04	-5.9E-03	3.7E-05	1.5E-04	-9.1E-06						

Table 4: Segment Racking - Segment Deformations

Segment	Segment	NODE	Deformation of Each Segment						Rigid Boody Motion of Each Segment					
SID	Name	ID	TX	TY	TZ	RX	RY	RZ	TX	TY	TZ	RX	RY	RZ
			in	in	in	rad	rad	rad	in	in	in	rad	rad	rad
	Focal	8101	-1.5E-05	-5.6E-05	2.7E-20	5.9E-05	7.9E-05	-5.2E-06	0.0E+00	0.0E+00	0.0E+00	0.0E+00	0.0E+00	0.0E+00
	Plane	8105	-4.1E-05	4.1E-05	-2.7E-20	-3.6E-05	6.9E-05	2.1E-06						
100		8110	5.6E-05	1.5E-05	-6.8E-21	2.2E-06	1.6E-04	3.1E-06						
	SEG101	8201	1.4E-04	-1.4E-04	-4.6E-04	5.0E-05	1.2E-04	-5.5E-06	4.1E-04	-2.4E-04	2.3E-03	5.1E-05	1.8E-04	9.0E-07
		8205	4.8E-04	-2.2E-04	-4.8E-03	7.1E-05	1.6E-04	1.0E-05						
101		8210	4.5E-04	-2.4E-04	-1.6E-03	4.4E-05	1.4E-04	-6.0E-06						
	SEG102	8301	-1.3E-04	-1.4E-04	5.7E-04	3.3E-05	7.6E-05	1.1E-05	1.5E-04	-1.9E-04	-1.5E-04	3.4E-05	3.0E-05	1.1E-05
		8305	-2.9E-04	-7.0E-05	9.1E-04	3.7E-05	4.1E-05	8.2E-06						
102		8310	-2.9E-04	-3.5E-04	1.6E-03	2.5E-05	4.6E-05	1.0E-05						
	SEG103	8401	-7.4E-05	-5.8E-05	4.5E-04	4.3E-06	8.5E-05	-9.3E-06	-4.2E-05	-3.3E-04	-2.1E-03	4.9E-05	1.1E-04	-1.1E-05
		8405	3.6E-04	-5.6E-06	2.8E-03	4.2E-05	8.9E-05	-2.1E-05						
103		8410	1.2E-04	1.3E-04	3.1E-03	1.6E-05	1.0E-04	-5.7E-06						
	SEG104	8501	-4.0E-05	2.1E-04	1.8E-03	-4.7E-05	1.2E-04	-3.6E-06	1.0E-04	3.3E-04	-8.6E-04	-8.1E-05	9.5E-05	2.4E-07
		8505	1.5E-04	3.6E-04	4.0E-03	-7.7E-05	1.0E-04	5.9E-06						
104		8510	1.6E-04	3.5E-04	4.6E-03	-7.0E-05	1.2E-04	-1.4E-06						
	SEG105	8601	1.0E-04	8.8E-05	1.3E-05	-7.9E-06	1.4E-04	1.5E-05	9.5E-05	1.0E-04	-1.7E-04	-8.6E-06	1.5E-04	1.0E-05
		8605	6.0E-04	-1.1E-05	1.9E-03	-3.3E-06	1.5E-04	1.1E-05						
105		8610	6.0E-04	2.3E-04	-1.6E-03	-8.3E-06	1.5E-04	1.2E-05						
	SEG106	8701	2.2E-04	-4.6E-05	-2.3E-03	3.4E-05	1.7E-04	-7.7E-06	5.8E-04	1.1E-04	1.0E-03	3.3E-05	1.6E-04	-1.1E-05
		8705	3.1E-04	-2.3E-04	-5.0E-03	3.3E-05	1.7E-04	-1.4E-05						
106		8710	5.4E-04	-3.8E-04	-6.2E-03	3.8E-05	1.6E-04	-9.1E-06						

The nodal deformations after the removal of the individual segment rigid body motion, are shown in Table 5. These residual deformations are the change in shape or racking of the interface triads. It is these values that represent the portion of the total deformation that would actually distort and strain the optical element. Essentially the racking algorithm provides a tool to evaluate and separate the total deformation into sets of physically meaningful quantities. These can include the rigid body of the assembly or a defined reference on the assembly and the deformation of individual subassemblies, including both rigid body motion and resulting racking of the subassembly.

Table 5: Segment Racking – Residual Racking Deformations

Segment SID	Segment Name	NODE ID	Residiual Racking Deformation of Each Segment					
			TX	TY	TZ	RX	RY	RZ
			in	in	in	rad	rad	rad
	Focal Plane	8101	-1.5E-05	-5.6E-05	2.7E-20	5.9E-05	7.9E-05	-5.2E-06
		8105	-4.1E-05	4.1E-05	-2.7E-20	-3.6E-05	6.9E-05	2.1E-06
100		8110	5.6E-05	1.5E-05	-6.8E-21	2.2E-06	1.6E-04	3.1E-06
	SEG101	8201	7.1E-07	7.1E-06	3.7E-07	-9.6E-07	-5.4E-05	-6.4E-06
		8205	4.0E-06	-9.7E-07	2.6E-07	2.0E-05	-2.1E-05	9.3E-06
101		8210	-4.7E-06	-6.2E-06	-6.4E-07	-7.2E-06	-3.6E-05	-6.9E-06
	SEG102	8301	-9.8E-06	2.4E-06	2.2E-07	-9.1E-07	4.6E-05	4.4E-07
		8305	5.4E-06	7.2E-06	6.4E-07	3.2E-06	1.0E-05	-2.7E-06
102		8310	4.4E-06	-9.6E-06	-8.6E-07	-8.4E-06	1.6E-05	-4.1E-07
	SEG103	8401	5.3E-06	-5.2E-06	-6.4E-07	-4.5E-05	-2.7E-05	2.0E-06
		8405	-4.4E-06	2.8E-06	4.6E-07	-6.9E-06	-2.3E-05	-9.9E-06
103		8410	-9.4E-07	2.4E-06	1.8E-07	-3.3E-05	-1.2E-05	5.7E-06
	SEG104	8501	-1.1E-05	-2.7E-06	9.6E-07	3.5E-05	2.7E-05	-3.8E-06
		8505	4.5E-06	8.2E-06	-7.2E-07	4.5E-06	7.0E-06	5.7E-06
104		8510	6.3E-06	-5.5E-06	-2.4E-07	1.1E-05	2.0E-05	-1.6E-06
	SEG105	8601	-7.6E-06	-3.0E-06	2.7E-07	6.9E-07	-2.5E-06	4.4E-06
		8605	3.1E-06	8.1E-06	-7.2E-07	5.3E-06	1.6E-06	5.6E-07
105		8610	4.6E-06	-5.1E-06	4.5E-07	3.1E-07	-1.2E-06	1.3E-06
	SEG106	8701	-1.5E-05	7.9E-07	-1.2E-06	1.0E-06	5.4E-06	3.5E-06
		8705	5.8E-06	8.4E-06	7.4E-08	8.5E-07	7.6E-06	-3.0E-06
106		8710	8.9E-06	-9.2E-06	1.1E-06	5.7E-06	7.8E-07	2.0E-06

3.2 Racking Analysis as an Aid to Model Correlation

Model correlation involving the comparison of physical measurements and FE predictions can be difficult. Modern measurement tools such as Laser Trackers or photogrammetry can provide numerous and accurate measurements of a distorted structure. The individual measurements actually represent a distance from the measurement device to the point on the object being surveyed. Given that the desired output is actually the distortion of the object, post processing of the individual measurements typically involves selecting a reference on the object and performing a best-fit calculation to determine the distances relative to the reference. This identical process can be completed using the FE results. The raw deformations of the FEM define the total motion of a point in an absolute frame of reference that is inaccessible to the hardware measurement process. By utilizing the segment racking technique, deformations relative to the reference comparable to the measurement results are easily determined. These values represent the identical output of the physical measurement process greatly simplifying the prediction/measurement correlation.

This capability has been very valuable in the process of assembly and integration of segmented optical systems. The process of assembly can be predicted by a piecewise linear analysis in which constraints to ground and between nodes are turned on and off in a sequence that mimics the successive integration of multiple assemblies.[6] The resulting analysis results show the development of built in strain associated with integration in a 1g environment. The analysis process may be used to develop and validate an assembly process that will meet requirements. Trade studies can involve consideration of offloading techniques and order of integration. Subsequently, during the process of hardware integration the racking results from SigFit can be used in real time to compare to observed racking measurements to ensure that the assembly process is progressing as predicted by the analysis.

3.3 Racking Analysis as an Aid to Visualization of Segment Deformation

Very often in the mechanical analysis of array systems the deformation of segments contains significantly more rigid body motion than elastic deformation. This makes it very difficult to see the elastic deformation of segments with unprocessed finitelement results in a post-processing application. This effect is demonstrated in Figure 9. Figure 9(a) shows the total deformation of the segment including the rigid body motion while Figure 9(b) shows the segment level racking deformation clearly showing the elastic component of deformation.

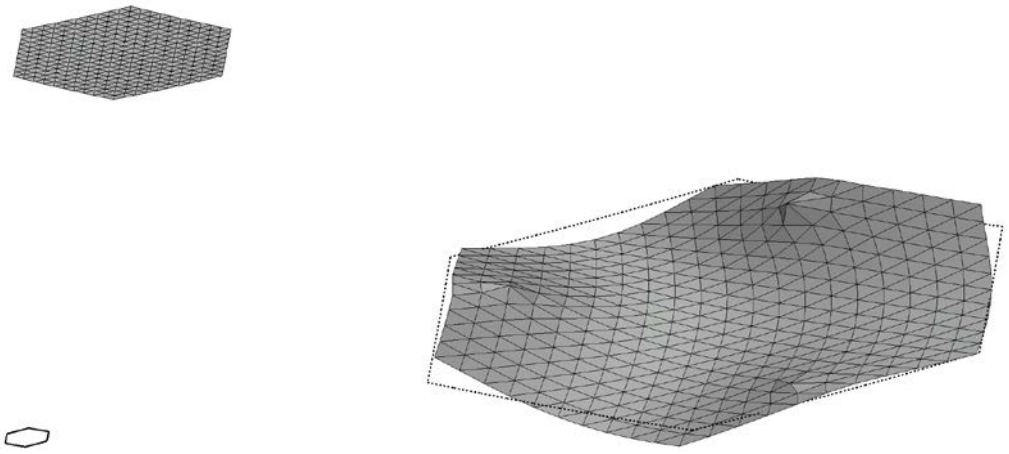

(a) (b)

Figure 9: Illustration of enhanced visualization of elastic deformation through segment level racking analysis: (a) total deformation of segment including rigid body motion and (b) segment level racking deformation more clearly showing elastic deformation.

With such visualization an assessment of how the segments are deforming may be understood in order to assist design development and performance improvement.

4. CONCLUSION

Analysis capabilities unique to the support of the analysis of segmented astronomical systems have been developed. The techniques employed allow relevant performance characterization and visualization of the behavior of such systems as well as tools to help direct design development for improvement in performance. The techniques discussed are also useful in transforming raw analysis results into forms comparable to measured test data during assembly procedures and in visualizing elastic deformation predictions without the masking effects of relatively significant rigid body motion.

REFERENCES

[1] Genberg, V., et. al., "Integrating MD Nastran with optical performance analysis," Proc. MSC Nastran User Conference, (2011).

[2] Doyle, K. B. et. al., "Optical modeling of finite element surface displacements using commercial software," Proc. SPIE 5867-18, (2005).

[3] SigFit is a commercial software product and trademark of Sigmadyne, Inc.

[4] Michels, G. J., et. al., "Analysis techniques for adaptively controlled segmented mirror arrays," Proc. SPIE 8447, (2012).

[5] Doyle, K. B., et. al., **Integrated Optomechanical Analysis**, 2nd ed., SPIE Press, (2012).

[6] Stone, M.J., V.L. Genberg, "Nonlinear superelement analysis to model assembly process," Proceedings of MSC World Users Conference, (1993).